[29] Fluorescent Protein-Based Cellular Assays Analyzed by Laser-Scanning Microplate Cytometry in 1536-Well Plate Format

By DOUGLAS S. AULD, RONALD L. JOHNSON, YA-QIN ZHANG, HENRIKE VEITH, AJIT JADHAV, ADAM YASGAR, ANTON SIMEONOV, WEI ZHENG, ELISABETH D. MARTINEZ, JOHN K. WESTWICK, CHRISTOPHER P. AUSTIN, and JAMES INGLESE

Abstract

Microtiter plate readers have evolved from photomultiplier and charged-coupled device-based readers, where a population-averaged signal is detected from each well, to microscope-based imaging systems, where cellular characteristics from individual cells are measured. For these systems, speed and ease of data analysis are inversely proportional to the amount of data collected from each well. Microplate laser cytometry is a technology compatible with a 1536-well plate format and capable of population distribution analysis. Microplate cytometers such as the Acumen Explorer can monitor up to four fluorescent signals from single objects in microtiter plates with densities as high as 1536 wells. These instruments can measure changes in fluorescent protein expression, cell shape, or simple cellular redistribution events such as cytoplasmic to nuclear translocation. To develop high-throughput screening applications using laser-scanning microplate cytometry, we used green fluorescent protein- and yellow fluorescent protein-expressing cell lines designed to measure diverse biological functions such as nuclear translocation, epigenetic signaling, and G protein-coupled receptor activation. This chapter illustrates the application of microplate laser cytometry to these assays in a manner that is suitable for screening large compound collections in high throughput.

Introduction

Cell-based fluorescent assays that use green fluorescent protein (GFP) as a reporter are a well-validated format for measuring a variety of biological phenomenon (Shaner *et al.*, 2005; van Roessel and Brand, 2002). The adaptation of these systems to microtiter plates has been a central goal within the biopharmaceutical industry because the microtiter plate is the standard container format for compound screening (Carroll *et al.*, 2004). A challenge for some instrument developers has been to accommodate the use of high-density microtiter plates, such as the 1536-well plate. Application of

0076-6879/06 $35.00
DOI: 10.1016/S0076-6879(06)14029-X

GFP-based cellular assays to large-scale compound screening depends on a robust and stable signal from the GFP reporter and high-throughput handling and reading of microtiter plates. The use of GFP detection in 1536-well plates enables the large-scale screening of compound collections against a diverse number of optimized GFP cell lines now available.

Using laser-scanning cytometry, we developed methodologies to screen three cellular assays based on inherently fluorescent GFP or fragments based on GFP variants (Fig. 1A). The first is a Redistribution assay (BioImage A/S) in which a glucocorticoid receptor–GFP (GR-GFP) fusion

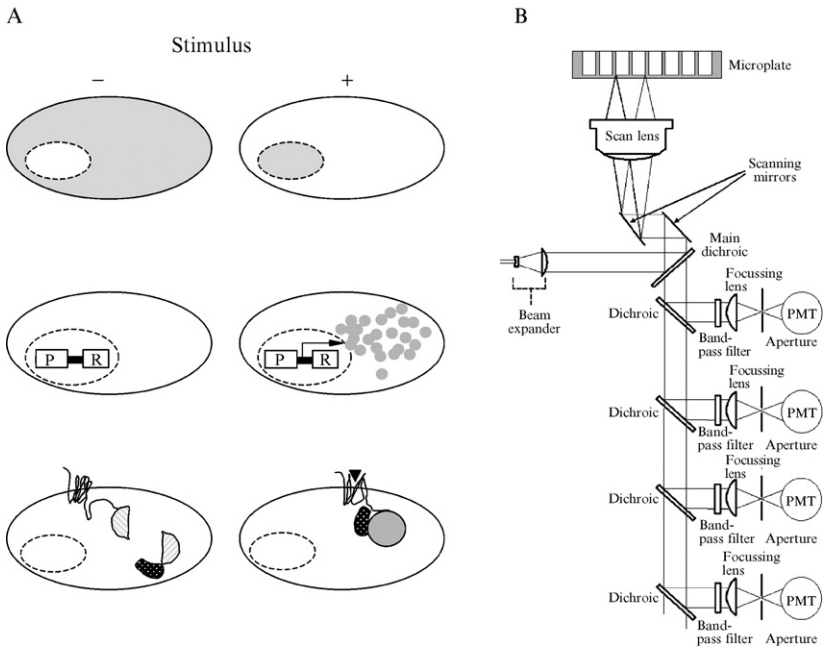

FIG. 1. Principles of fluorescent protein-based cell assays and configuration of laser optics within the Acumen Explorer. (A) GFP fusion proteins can be constitutively produced and their subcellular distribution modulated as in the GR-GFP assay where cytosolic GR-GFP is translocated into the nucleus upon ligand binding (top). GFP production can report transcriptional activation as in the LDR assay where derepression of a transcriptionally silent locus induces GFP expression (middle). Nonfluorescent fragments of YFP can interact noncovalently to reconstitute fluorescence as in the βARR:β2AR assay where fragments fused to interacting partners, β-arrestin and β_2-adrenergic receptor, associate upon receptor stimulation (bottom). (B) Laser light is directed to the F-theta scan lens by a dichroic beam splitter and galvanometric mirrors. The scan lens focuses the light onto the microplate bottom, and the resulting epifluorescence is directed to four PMT detectors by a series of mirrors and dichroics. Band-pass filters select specific ranges of wavelengths for each PMT. Galvanometric mirrors guide the laser line across a 20-mm^2 area at 5 m/s (diagram adopted from Bowen *et al.*, 2006).

is used to measure ligand-dependent translocation from the cytoplasm to the nucleus in U2OS cells (Jung-Testas and Baulieu, 1983; Levinson *et al.*, 1972). The second, a locus derepression (LDR) assay, is a mouse mammary cell line, derived from C127 cells, where GFP is stably integrated into a transcriptionally silent region of the genome. Compounds that activate this chromosomal locus (loci) can be identified by enumerating GFP-positive cells after treatment. The third is a protein fragment complementation assay (PCA) in HEK293T cells whereby fragments of an intensely fluorescent YFP mutant are fused to the β-adrenergic G protein-coupled receptor and β-arrestin. Following activation of the β-adrenergic receptor, the association of β-arrestin enables yellow fluorescent protein (YFP) fragment association, folding, and generation of a fluorescent signal (MacDonald, 2006; Remy and Michnick, 2003; Yu *et al.*, 2003).

The Principle of Laser-Scanning Microplate Cytometers

Current microplate readers vary with respect to their speed of plate reading and the amount of information that is extracted. On one end of the spectrum are very fast plate readers such as the ViewLux (Perkin Elmer), a cooled charge-coupled device (CCD)-based imager that captures plate data in under a minute for typical luminescence or fluorescence assays. Imagers such as these offer the additional advantage of data collection speed that does not depend on the plate well density. However, such readers only measure the total signal arising from the cell population in each well. Additionally, the excitation source and detection systems in such readers are not sufficiently sensitive to reliably measure weakly fluorescent molecules such as GFP (unpublished observations).

On the other end of the spectrum are high-content screening (HCS) imagers, such as the ArrayScan (Cellomics, Inc.; see, e.g., Williams *et al.*, 2006), the Opera (Evotec; see, e.g, Garippa *et al.*, 2006), the Pathway BioImager (BD Biosciences; see, e.g,, Richards *et al.*, 2006), and the IN Cell imagers (GE Healthcare; see, e.g., Haasen *et al.*, 2006) that capture high-resolution images in subcellular detail from numerous cells per well. While HCS readers provide a wealth of data on every well, they have relatively slow scan times compared to population-averaged readers, generate large data files (MB per well are common), and data collection speeds are dependent on plate well density.

Between these two approaches resides the laser-scanning microplate cytometer that images fluorescent beads or cells within microtiter wells independent of microscope optics. The latest generation of these instruments is the Acumen Explorer (TTP Labtech) that provides read times sufficient for high-throughput screening (HTS) (up to 300,000 samples per

day in 1536-well plates) while making multiparameter measurements on individual cells or other micrometer size particles (Bowen and Wylie, 2006).

The Acumen Explorer collects data by focusing a laser excitation beam on the bottom of the microtiter plate and collecting the resulting epifluorescence using photomultiplier tubes (PMT) for specific wavelength ranges (Fig. 1B). Fluorescent characteristics of individual objects can then be characterized and enumerated into various populations. The 488-nm laser is optimal for excitation of GFP-based assays, and the optics and plate positioning are sufficiently fast to read a 1536-well plate in approximately 10 min (200 whole-well scans/minute at 1×8-μm resolution). The resolution along the x axis is set at predetermined intervals (0.1, 0.5, 1, 2.5, or 5 μm) while the y axis is set by the user, typically between 1 and 10 μm.

The amount of image data saved is determined by the need of the process; for identifying the critical object characteristics of an assay phenotype, the assay development mode is used to capture high-density information. However, for screening, the HTS mode is used to collect only the critical assay parameters, thereby reducing the file size by several hundredfold (<200 KB for 1×8 μm whole well scan of a 1536-well plate). As plate file size is kept small, microplate cytometers facilitate HTS of large chemical libraries against various cell-based assays. The methods for performing 1536-well assays using the Acumen Explorer, as well as proof-of-principle screening data, are shown next.

General Methods

Preparation of the Library of Pharmacologically Active Compounds (LOPAC) Titration Series

The LOPAC 1280 (Sigma Aldrich) collection is screened as a series of interplate titrations to generate concentration–response curves for each compound. The generation of titration–response curves enables accurate assessment of the AC_{50} of each compound (concentration for half-maximal activity) and eliminates false positives and negatives (Inglese, 2006).

The collection is received in 96-well tube plates as dimethyl sulfoxide (DMSO) solutions at 10 mM and compressed into 384-well Kalypsys polypropylene plates via interleaved quadrant transfer using a CyBi-Disk Vario system equipped with a 96-tip head (CyBio AG). Titration and subsequent compression of 384-well plates to 1536-well plates are performed by an Evolution P^3 (Perkin Elmer). In the final 1536-well plates, the four left-most columns are unfilled. Fifteen 2.24-fold and seven 5-fold dilutions of the LOPAC library are prepared with each plate containing a copy of the library at successive dilutions. For long-term storage, plates are

heat sealed on a PlateLoc thermal plate sealer equipped with a BenchCell 2× stacker system (Velocity 11). For a more detailed description of library preparation, see Inglese (2006).

Configuration of the Acumen Explorer

The Acumen Explorer uses a 25-mW argon laser as an excitation source and four PMTs that collect the following emission wavelengths: channel 1, 500–530 nm; channel 2, 530–585 nm; channel 3, 575–640 nm; and channel 4, 655–706 nm. The instrument is controlled by a Hewlett Packard Intel XEON CPU (1.8 GHz) workstation containing 3 GB of RAM and a MDAQ data acquisition card. In this configuration, the maximum scan speed is 10 m/s with a maximum sampling rate per channel of 10 MHz.

1536-Well Plate Liquid Handling

Cell suspensions are dispensed into 1536-well plates using a Flying Reagent Dispenser [FRD, Aurora Discovery (Niles and Coassin, 2005)] or a Kalypsys 1536-well plate washer/dispenser. These dispensers use pressurized bottles (6 to 9 psi) to dispense liquid through a solenoid valve and can accurately dispense volumes as low as 1 μl. Bulk reagent addition and aspiration are performed using a Kalypsys washer/dispenser.

The compound is transferred by a Kalypsys pin tool workstation equipped with 1536 10-nl slotted pins [0.457 mm diameter, 50.8 mm long; VPN Scientific (Cleveland and Koutz, 2005)]. The pin-tool transfer is validated using fluorescein-containing DMSO solution that confirms transfer of 23 nl from the compound plate to an assay plate containing 5 μl of buffer. The pin transfer protocol for cell-based assays uses one pin immersion in the compound plate and three immersions in the assay plate, with the pins not touching the assay plate bottom to avoid disrupting the cell monolayer. For screening, two compound plates are transferred to each assay plate, one containing library compounds followed by one containing assay-specific controls. For all incubations, assay plates are lidded with stainless-steel Kalypsys plate lids that contain a rubber gasket to seal the edges of the plate and pin holes across the middle of the plate allow gas exchange (Mainquist, 2003).

The Kalypsys washer/dispenser has a 32-channel stainless-steel head to aspirate an entire column from 1536-well plates. Aspiration depends on several factors: the vacuum flow level, the aspiration-tip well depth, and the dwell time. The vacuum flow level is controlled by manually adjusting a needle valve that on our instrument is opened two full turns. The aspiration well depth is set to 2.75 mm from the top of the well and the dwell time to 200 ms. These settings result in 1.5 μl/well of residual liquid as determined by gravimetric measurement of test plates. At the start and finish of all

procedures, the aspirator head is cleaned by a 5-min aspiration of 10% bleach followed by distilled water. If the head is used frequently, then at least once per month, remove the head, soak overnight in Coulter Clenz (Coulter Corporation), and then sonicate for several hours.

The accuracy and precision of the aspirator head are tested as follows: 5 μl/well of 5 μM fluorescein in buffer is dispensed into a tared 1536-well plate, the plate is weighed, and the fluorescent signal is measured by a plate reader. The coefficient of variation (CV) of the plate should be below 5%. Following one wash cycle, the residual volume is checked gravimetrically and the CV is measured by plate reader. The CV should be below 10% following a single aspiration cycle.

Data Processing

Screening data are corrected and normalized using Assay Analyzer (GeneData). Control assay plates containing vehicle (DMSO) only are used to monitor background systematic variation. Correction factors are generated from these variations and applied to each assay plate to correct systematic errors. Percentage activity is calculated by normalization to the median values of the activator and neutral controls present on each plate. Plate and compound mapping is performed to correlate percentage activity with the corresponding concentration for each sample to generate a titration-response series for each compound. Concentration–response graphs are displayed using Prism (Graph Pad) and Origin (OriginLab).

GR-GFP Nuclear Translocation Assay

The glucocorticoid receptor (GR) Redistribution assay enables the visualization of GR cytoplasmic to nuclear translocation by the use of a GR-GFP fusion (BioImage). GR is normally cytosolic; however, ligands such as dexamethasone cause nuclear translocation where the protein binds to response elements and interacts with various cofactors to modulate transcription (Bai *et al.*, 2003; Zhou and Cidlowski, 2005). Because both functional agonists and antagonists can induce nuclear translocation (Htun *et al.*, 1996), this assay can detect ligands regardless of their effects on gene expression. For this reason, the measurement of nuclear translocation is a desirable assay for broadly screening compound libraries for nuclear receptor ligands.

Solutions and Materials

GR-GFP expressing U2OS cells are maintained in DMEM with Glutamax and high glucose (Invitrogen), 1% (v/v) penicillin–streptomycin (Invitrogen), and 0.5 mg/ml Geneticin (Invitrogen). For cell culture, 10%

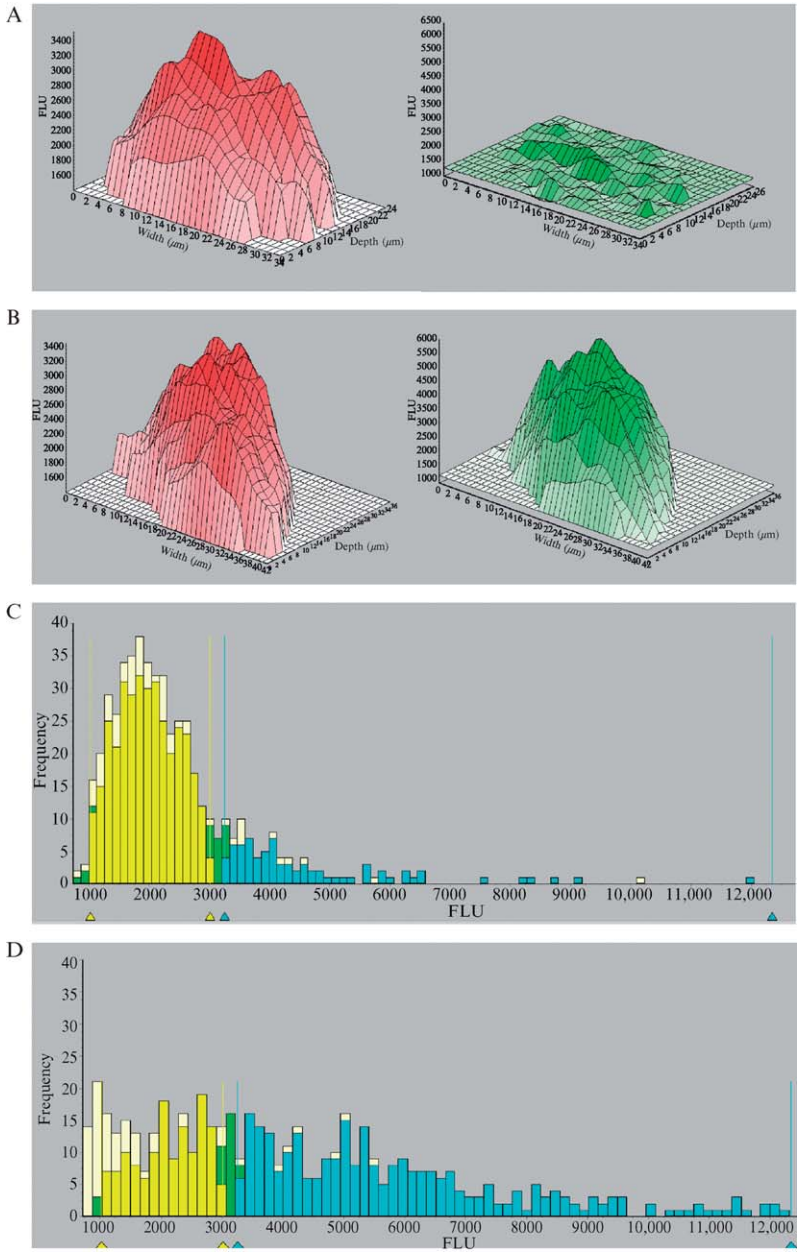

FIG. 2. Three-dimensional representation and population histogram of translocated and untranslocated objects from the GR-GFP assay. The PI (red) and GFP (green) signals of a

heat-denatured fetal bovine serum (FBS) is used (Invitrogen). For cell plating, 10% dextran, charcoal-stripped FBS (Hyclone SH30068.03) is used. Dimethyl sulfoxide, certified A.C.S. grade, is from Fisher. Black polystyrene, clear-bottom, 1536-well plates (#K1536SBCN, Hi Base plates) are manufactured by Greiner and purchased from Kalypsys. Propidium iodide (PI) is from Molecular Probes. Dexamethasone is from Calbiochem.

High-Throughput Screening Protocol

1. U2OS cells are trypsin treated, suspended in medium, and passed through a 40-μm basket filter (BD Falcon). The cells are seeded at 600 cells/5 μl/well into 1536-well plates and incubated for approximately 20 h at 37° and in 5% CO_2.
2. The compound is transferred to assay plates by pin tool, resulting in a 217-fold dilution of compound and 0.4% DMSO final concentration. The control plate contains a titration of dexamethasone in the first two columns (starting at 0.2 m*M* and diluting by 2-fold for 16 rows), DMSO in the third column, 0.2 m*M* dexamethasone in the fourth column, and the remaining columns are empty.
3. The assay plates are incubated at 37° in 5% CO_2 for 2 h.
4. Cells are fixed using the Kalypsys washer/dispenser. The protocol involves aspiration of the cell media, addition of 6 μl/well of phosphate-buffered saline (PBS), aspiration of PBS, addition of 5 μl/well of 100% methanol, aspiration of methanol, and addition of 3 μl/well PBS with 1.5 μ*M* PI.
5. The plates are read by the Acumen Explorer using the following settings: 6 mW laser power, 650 and 690 V for the GFP (channel 1) and PI (channel 3) PMTs, respectively, 2 standard deviations (SD) above background fluorescence threshold for data collection, and 1×4 μm[1] scan of the whole well area. PI fluorescence triggers the collection of PI and GFP signals. A ''nuclei'' population is defined by a 10- to 100-μm width and depth filter that eliminates small and large fluorescent particles (Fig. 2). Two subpopulations

[1] We have obtained equivalent data with 1×8-μm scans.

nucleus within an untreated cell (A) and a cell treated with 50 n*M* dexamethasone (B) are shown. Histograms depicting object number versus fluorescent intensity for untreated (C) and dexamethasone-treated cells (D). Nuclei were classified as objects between 10 and 100 μm width and depth. Objects outside this size range are shaded pale yellow. Nuclei subpopulations were categorized by the level of GR-GFP fluorescence (translocated, blue; untranslocated, yellow; and unclassified, green).

A
DMSO
0.6 nM
1.3 nM
3 nM
6.6 nM
14.7 nM
DMSO
33 nM
74 nM
165 nM
368 nM
824 nM
DMSO
1.8 μM
4.1 μM
9.2 μM
20.6 μM
46 μM
DMSO
Activity scale
0
100
B
S/B
Z′
Plate #
C
% Activity
Log [dexamethasone]
D
Sample
Log [compound]
% Activity

of ''nuclei'' are defined by peak intensity of GFP fluorescence, where translocated objects are between 4000 and 15,000 fluorescence units (FLU) and untranslocated objects are between 1000 and 3999 FLU.

Validation of the 1536-Well GR Nuclear Translocation Assay

To validate the 1536-well protocol, we screened the LOPAC library that contains known glucocorticoid and steroidal agonist and antagonists. Nineteen 1536-well plates were run in one batch (Fig. 3A). With the optimized protocol, we obtained a 10% CV for the number of nuclei/well, indicating there was little spurious loss of cells from plate washing. The Z' calculated from the enumerated translocated objects averaged approximately 0.3 with a signal to background (S/B) of 6 (Fig. 3B). Intraplate dexamethasone titrations also showed reproducible performance with an average AC_{50} of 6 nM (Fig. 3C), in agreement with published observations (Martinez *et al*., 2005). Displaying the entire titration-based screen as a scatter plot revealed the presence of wells with spurious high values (Fig. 3D). However, as the LOPAC library was screened as titration, artifacts showing a response at a single concentration were easily distinguished from genuine actives that showed a concentration–response relationship.

Example concentration–response curves obtained from the screen were of high quality (Fig. 4). Twenty-seven actives were identified with an AC_{50} under 12 μM. All 10 compounds annotated as glucocorticoids in the LOPAC collection[2] were found as actives, including both agonists and antagonists. At the higher concentrations, additional classes of active compounds were found that included compounds annotated as phosphatase inhibitors and G protein-coupled receptor (GPCR) ligands. These compounds could be targeting pathway components involved in GR function or translocation.

[2] LOPAC annotates 34 compounds as nuclear receptor hormone ligands with 10 of these annotated as glucocorticoids, including cortisol and its analogs.

FIG. 3. Validation screen of the LOPAC library against the GR-GFP assay. (A) A heat map is shown of the LOPAC library screened at 15 concentrations plus four DMSO blanks used for background correction. Carryover of potent library compounds into the DMSO plates can be seen. Controls are arrayed on the left side of each plate. (B) Average S/B and Z' calculated from control wells for all plates. (C) Titration–response curves for the dexamethasone control present on all plates indicated an average AC_{50} of 6 nM. (D) A three-dimensional scatter plot displaying inactive (black) and active (red) samples that showed a concentration–response relationship.

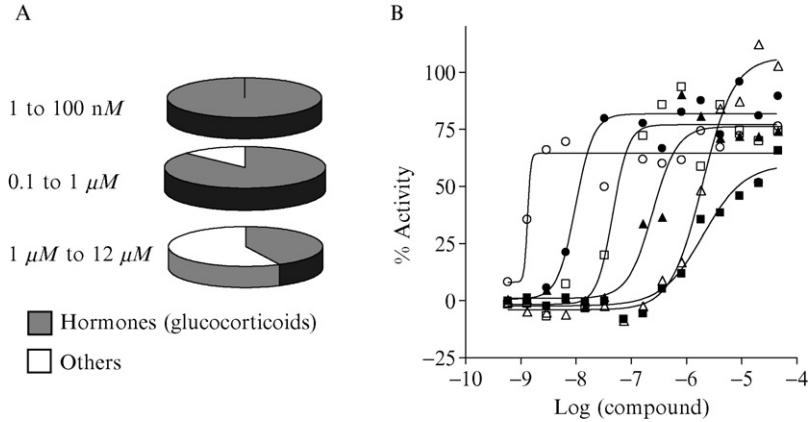

FIG. 4. Results of the LOPAC screen against the GR-GFP assay. (A) LOPAC annotation of glucocorticoid (shaded) and nonglucocorticoid (unshaded) actives identified in the GR-GFP screen binned by AC50: 1 to 100 nM ($n = 5$), 0.1 to 1 μM ($n = 8$), 1 to 12 μM ($n = 14$). (B) Example concentration–response curves obtained from the screen: LOPAC-B-7777 (budesonide, ○), LOPAC-H-4001 (hydrocortisone, ●), LOPAC-S-3378 (spironolactone, □), LOPAC-T-6376 (fluoxyprednisolone, ▲), LOPAC-B-7880 (8-bromo-cAMP, △), and LOPAC-H-2270 (hydrocortisone 21, ■).

Locus Derepression Assay

The LDR assay detects the derepression of a GFP reporter that is stably integrated in a transcriptionally silent region of the mouse genome (see Chapter 2, this volume). In the vector, GFP transcription is controlled by a CMV promoter, which normally is strong and constitutively active. However, this line was selected for lack of constitutive expression of the GFP reporter presumably due to epigenetic silencing of the integration locus and/or methylation of the CMV promoter, which contains a large CpG island. GFP transcription can be induced by incubating the cells with histone deacetylase (HDAC) inhibitors such as butyrate or trichostatin A (TSA), which remodel the chromatin from a closed to open conformation to allow transcription (Thiagalingam *et al.*, 2003) or with inhibitors of DNA methyltransferases such as 5-aza-deoxycytidine. A more thorough discussion of this cell line and assay can be found in Martinez *et al.* (2006).

In the LDR assay, activity is measured by the number of GFP-positive cells in each well, where cells show little or no fluorescence without treatment, but many cells become fluorescent after treatment with HDAC inhibitors (Fig. 5). We used this assay to screen for compounds that induce GFP in the absence of HDAC inhibitors. This approach has the advantage of detecting an increase in signal (the number of positive GFP cells) from a

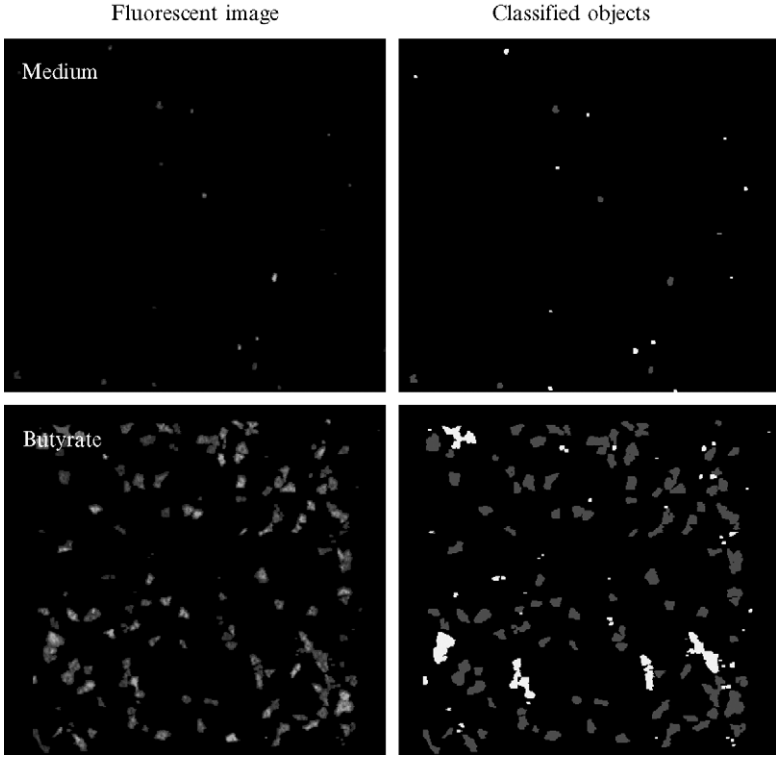

FIG. 5. Classification of GFP-positive cells in the LDR assay. Cells in a 1536-well plate were treated with culture medium minus (top) or plus (bottom) 25 m*M* sodium butyrate for 29 h at 37°, washed twice with PBS, and imaged by the Acumen Explorer. Live (left) and false-colored (right) images of a representative well treated with medium or butyrate are shown. Objects classified between 20 and 120 μm in width and depth are shaded gray, whereas objects outside this range are shaded white.

very low background and therefore the number of false positives is low. Furthermore, cytotoxic compounds are not identified, as dead or dying cells will not induce GFP production. Hence, the screen is very selective for compounds that are specific activators of GFP expression.

Assay Optimization for 1536-Well Plate Format

For the LDR assay to be sensitive, the GFP signal must be strong, the background fluorescence low, and the number of GFP-positive cells high. To achieve this sensitivity in a 1536-well plate format, several parameters required optimizing: cell density, incubation time, and cell preparation for imaging.

Cell density was optimized in order for the Acumen Explorer to accurately score individual cells within a well. GFP-positive cells were classified as fluorescent objects between the size of 20 to 120 μm width and depth. This filter selects objects in the size range of single cells to clusters of 2 to 3 cells. When too many cells are plated, cell foci form that are larger than the selected size range and are thus excluded from enumeration, resulting in fewer positive cells counted (Fig. 5). When too few cells are plated, single cells are mostly present but the total cell number is too low to differ significantly from background. For this assay, 250 to 300 cells/well in 1536-well plates yielded single cells or small cell clusters within the desired size range.

Several conditions were examined to determine the optimal imaging procedure. The simplest approach was to image live cells in medium following compound incubation, thus minimizing the number of steps in the protocol and reducing assay variability. Under these conditions, only the brightest GFP signals were detected and the resulting cell images appeared fragmented (Fig. 6). Because many of these image fragments were below the specified size range (20–120 μm width and depth), they were excluded from enumeration. This effect likely arises from fluorescent component(s) in the medium creating a high background that is then subtracted from the scan. Consequently, any low-level GFP signal arising from cells is also eliminated. While we have not identified the medium or cell components contributing to background fluorescence, phenol red, a medium constituent, is not the source (data not shown).

Image quality improved markedly following removal of the medium and two PBS washes (Fig. 6). Given that a brighter GFP signal was detected and the cell images were not fragmented, the number of cells enumerated increased by two thirds. The cell signal remained unchanged in PBS after 1 h at 37°, and even after an overnight incubation at 37°, the cells remained adherent and GFP positive, although the signal quality was diminished considerably (data not shown). Following PBS washes, cells could be fixed with methanol, although GFP fluorescence was lower and some cell images appeared fragmented (Fig. 6). While methanol fixation results in lower cell object counts, plates can be stored for later reading or reference.

The length of treatment time was optimized to determine the minimum incubation time to induce a strong GFP signal. Overnight incubation with sodium butyrate or TSA was sufficient to induce GFP but only in a minority of cells. Longer compound incubation times of 24 and 29 h with butyrate induced GFP at higher levels and in the majority of cells.

Solutions and Materials

C127-derived stably transfected mouse mammary cells are grown in DMEM with L-glutamine and high glucose (Invitrogen), 1 m*M* sodium

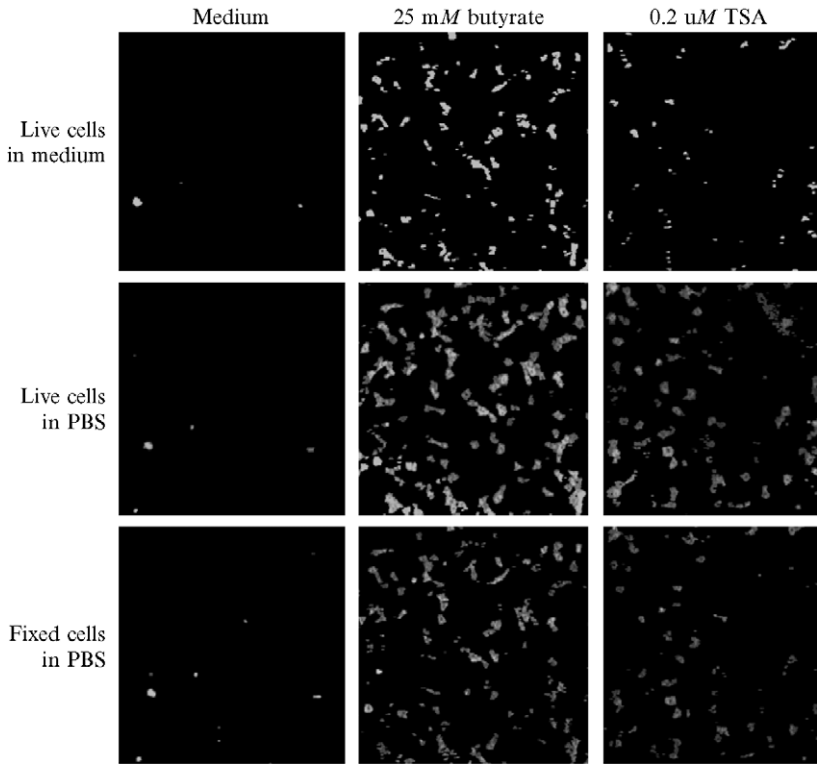

FIG. 6. Effect of wash conditions on LDR assay quality in a 1536-well plate format. Cells were treated with medium alone (left column), 25 m*M* sodium butyrate (middle column), or 0.2 μM trichostatin A (right column) for 24 h at 37°, and wells were imaged in culture medium (top row), after two PBS washes (center row), and after methanol fixation (bottom row). In each column, the same well is imaged following sequential wash and fix steps.

pyruvate (Invitrogen), 0.1 m*M* MEM nonessential amino acids (Invitrogen), 1% (v/v) penicillin–streptomycin (Invitrogen), and 10% heat-inactivated FBS (Hyclone). Sodium butyrate (Sigma-Aldrich) and TSA (Tocris) are used as positive controls.

High-Throughput Screening Protocol

1. Cells are harvested, passed through a 40-μm basket filter, and suspended at 50,000 cells/ml in growth medium. Cells are seeded at 250 cells/6 μl/well into black clear-bottom 1536-well plates using either a FRD or a Kalypsys dispenser.

2. The compound is transferred to assay plates by a pin tool. The control compound plate contains 16 2-fold titrations in duplicate of aqueous sodium butyrate beginning at 4.25 *M* in columns 1 and 2. Columns 3 and 4 contain water and 4.25 *M* sodium butyrate, respectively, and the remaining columns are empty. The final DMSO concentration is 0.4%, and the compounds are diluted by a factor of 261-fold upon transfer to the assay plate.

3. Assay plates are incubated for 30 h at 37° and 5% CO_2.

4. The medium is aspirated, and 6 μl/well of PBS is added and then replaced by a second dispense of 6 μl/well of PBS.

5. Plates are read in the Acumen Explorer using the following settings: 6 mW laser power, 660 V channel 1 PMT, 1 × 4 μm *x* and *y* scan resolution, 2.5 SD above background trigger threshold, 10-μm minimum and 100-μm maximum feature size, and sliding window of two kernel width and three kernel height for image filtering.

Validation of the 1536-Well LDR Assay

We screened the LOPAC compound collection to validate the LDR assay and characterize the number and potency of active compounds. The screen consisted of three DMSO control and seven LOPAC plates comprising a 5-fold titration series of 1280 compounds beginning at 10 μM. The signal quality across the screen was strong and stable; the S/B ranged from 66 to 199 and the Z' factor varied from 0.63 to 0.75 (Fig. 7C). Six compounds were identified as active at 10 μM and two of these showed activity at 2 μM as well (Fig. 7A and D). One identified active, 5-azacytidine, is an inhibitor of DNA methyltransferase, a known regulator of chromatin remodeling (Ben-Kasus *et al.*, 2005; Ghoshal *et al.*, 2002), indicating that the LDR assay is capable of finding known modulators of this biology. The LOPAC library does not contain known HDAC inhibitors.

β-Arrestin:β_2-Adrenergic Receptor (βARR:β2AR) Protein Fragment Complementation Assay

Protein fragment complementation assays involve two nonfluorescent GFP (or GFP variant) fragments fused to cellular proteins of interest. Upon noncovalent association of the cellular proteins, the GFP (or variant) fragments to which they are fused become fluorescent (MacDonald, 2006; Remy and Michnick, 2003; Yu *et al.*, 2003). PCA is applied to the association of β-arrestin with the β2AR whereby the C terminus of the β2AR is fused with one fragment of mutant YFP and β-arrestin is fused to the complementary fragment (Fig. 1A). Following agonist stimulation, the β2AR is

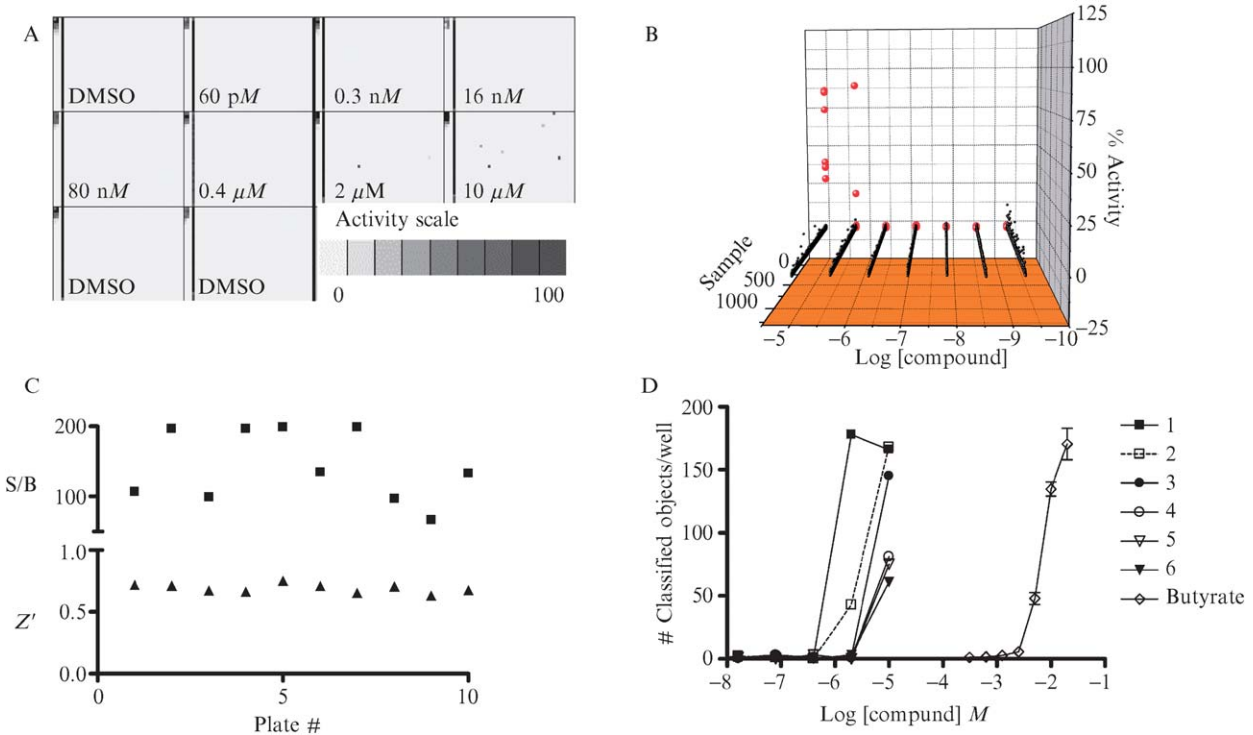

FIG. 7. Validation screen of the LOPAC library with the LDR assay. (A) A heat map depicts the LOPAC library screened at seven concentrations and includes three DMSO plates included for background correction. Controls are arrayed on the left side of each plate. (B) Three-dimensional scatter plot indicating inactive samples (black) and active (red) samples showing a concentration–response relationship. (C) Average S/B and Z' factor calculated from control wells for all plates. (D) Concentration–response plots of actives identified in the screen.

phosphorylated by GPCR kinases to cause enhanced association of the adaptor protein, β-arrestin (Ferguson *et al.*, 1998; Inglese *et al.*, 1993). In this assay, the β-arrestin and β2AR interaction enables association and folding of YFP fragments and generates a quantifiable fluorescence signal.

Solutions and Materials

βARR: β2AR cells are HEK 293T cells that stably express fusions of YFP fragments (Odyssey Thera, Inc.) maintained in DMEM with 10% FBS, 500 μg/ml of zeocin (Invitrogen) and 400 μg/ml of hygromycin B (Invitrogen). The agonist control, (−)-isoproterenol hydrochloride, the antagonist control, (*S*)-(−)-propranolol hydrochloride, and naphthol blue black are from Sigma-Aldrich.

Optimization of the 1536-Well Assay Protocol

Medium components can interfere with the fluorescence signal and image quality can be improved by removal of the medium (see LDR assay). βARR: β2AR cells are weakly adherent to tissue culture-treated microtiter plates and these cells cannot be washed by the Kalypsys washer/dispenser, even when grown on plates precoated with poly-L-lysine (data not shown). To circumvent the need of wash steps, a fluorescence-absorbing dye is added to decrease background fluorescence arising from the medium or unattached cells in the well. By reducing background fluorescence, the threshold value that triggers data collection (typically 2 SD above the background) is decreased and therefore the sensitivity of the fluorescence signal is increased. Cell density is kept to <700 cells/well to accurately measure background fluorescence between cells. The addition of 33 μ*M* naphthol blue black increases the S/B by approximately threefold (Fig. 8A).

High-Throughput Screening Protocol

1. Cells are suspended, passed through a 40-μm basket filter, seeded at 700 cells/5 μl/well into black clear-bottom 1536-well plates, and incubated for approximately 20 h at 37° and 5% CO_2.

2. Compound and control samples are transferred by a pin tool. The compound control plate contains 16 2-fold dilutions in duplicate of (−)-isoproterenol starting at 2 m*M* in column 1, 20 μ*M* (−)-isoproterenol (AC_{90}) in column 2, DMSO in the column 3, and 2 μ*M* (−)-isoproterenol (AC_{50}) in column 4. To screen for antagonists, columns 5 through 48 contain 2 μ*M* (−)-isoproterenol (AC_{50}) while when screening for agonists, these columns are empty. The final DMSO concentration is 0.5 % and the compounds are diluted 217-fold upon transfer to the assay plate.

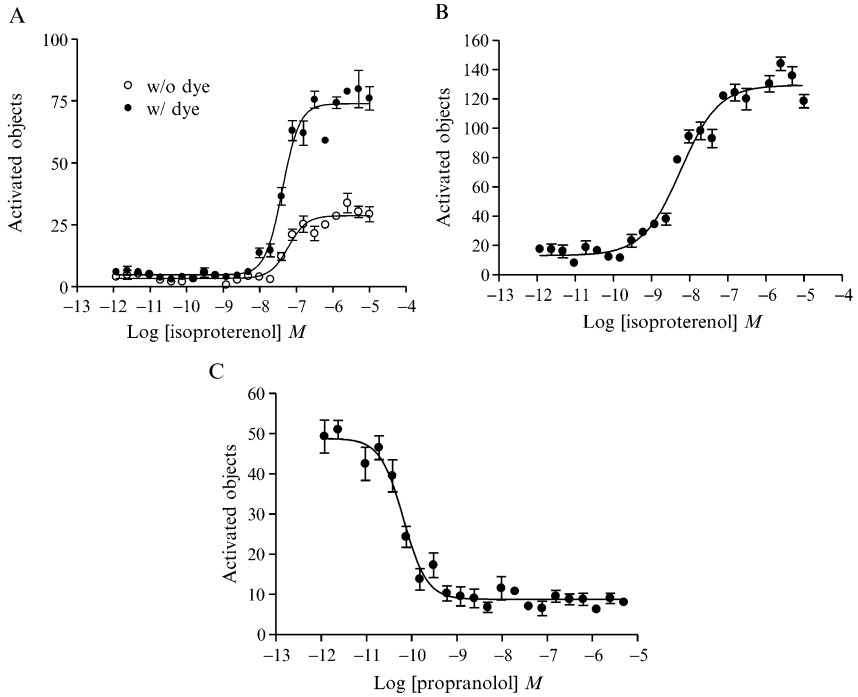

FIG. 8. Optimization of βARR:β2AR assay in agonist and antagonist formats in 1536-well plates. (A) Titration of isoproterenol in the presence or absence of 33 μM napthol blue black. Concentration–response curves for the agonist isoproterenol (B, AC_{50} = 6 nM) and the antagonist propranolol (C, AC_{50} = 60 pM) using the optimized 1536-well protocols. Cells were stimulated with 8 nM isoproterenol for the antagonist assay.

3. Assay plates are incubated at 37° and 5% CO_2 for 1.5 h.
4. One microliter per well of 0.2 mM naphthol blue black is added.
5. Plates are read by the Acumen Explorer using the following settings: 6 mW laser power, 630 V for the GFP (channel 1) PMT, 2 SD above background fluorescence threshold for data collection, and 1 × 8 μm scan of the whole-well area. Two populations, activated and unactivated, are defined by a 5- to 120-μm width and depth to eliminate small and large fluorescent particles. The activated population is classified as mean peak intensity between 1278 and 6185 FLU and total peak intensity between 21,408 and 154,242 FLU, while the unactivated population is defined as mean peak intensity between 230 and 1199 FLU and total peak intensity between 2684 and 18,464 FLU.

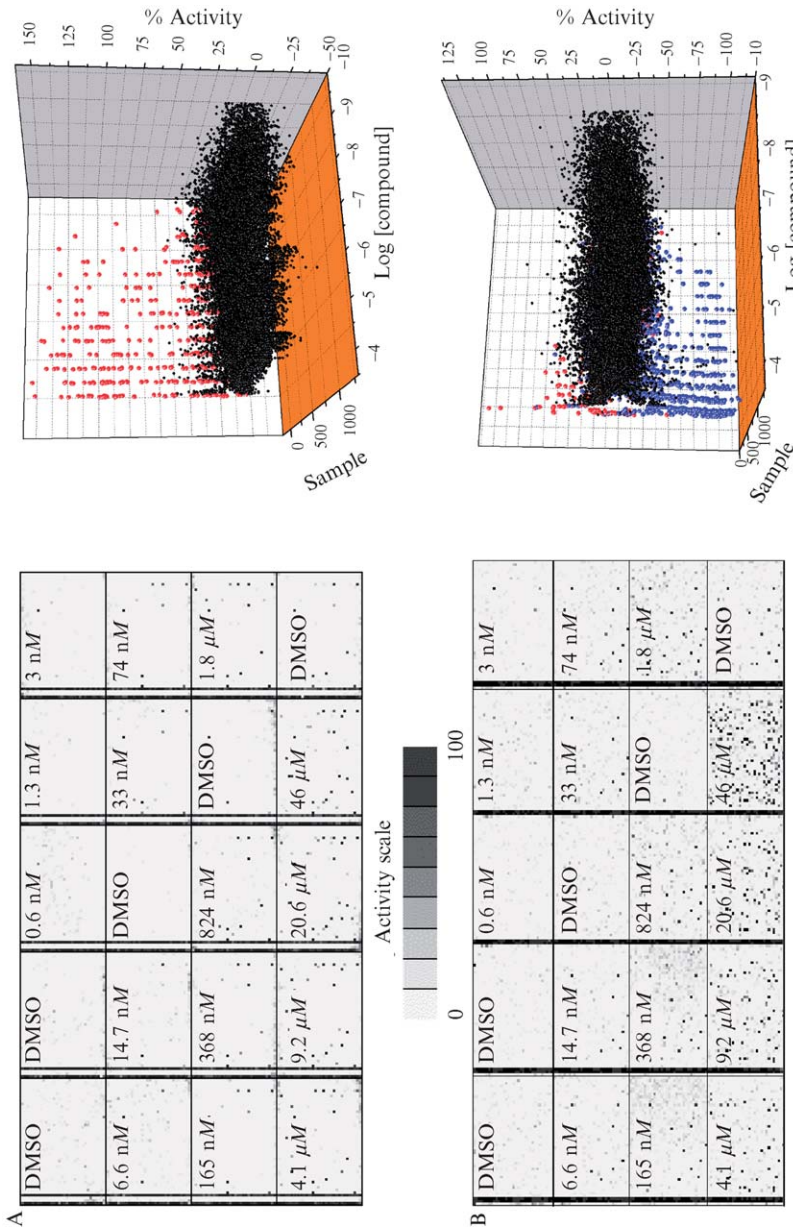
% Activity
Log [compound]
Sample
% Activity
Log [compound]
Sample
A
DMSO
DMSO
0.6 nM
1.3 nM
3 nM
6.6 nM
14.7 nM
DMSO
33 nM
74 nM
165 nM
368 nM
824 nM
DMSO
1.8 μM
4.1 μM
9.2 μM
20.6 μM
46 μM
DMSO
Activity scale
0
100
B
DMSO
DMSO
0.6 nM
1.3 nM
3 nM
6.6 nM
14.7 nM
DMSO
33 nM
74 nM
165 nM
368 nM
824 nM
DMSO
1.8 μM
4.1 μM
9.2 μM
20.6 μM
46 μM
DMSO

Assay Validation

The LOPAC library was screened against the βARR:β2AR assay in both agonist and antagonist formats (Fig. 9). Both assays showed suitable performance in high-throughput mode. The LOPAC library contains very potent adrenergic receptor ligands ($EC_{50} \sim 10$ n*M*) and for these, we observed some carryover from the pin tool on DMSO control plates (Fig. 9A and B). Because these assays were screened as a titration series, compound carryover did not complicate our analysis. However, if our assay protocol is used for single concentration screening of multiple library plates, improved pin washing will be needed.

The most potent compounds identified from the screens were known agonists or antagonists of the βAR (Fig. 10). The LOPAC library contains 47 agonists and 35 antagonists that are annotated as adrenergic receptor ligands. Of the 19 adrenergic receptor agonists identified with $AC_{50} \leq 10$ μ*M*, 18 are annotated as β-adrenergic agonists and one as an α-adrenergic receptor agonist. Twenty-five agonists, which were not identified at the 10 μ*M* AC_{50} threshold, are annotated as α- or β1/β3 adrenergic receptor agonists. For antagonists, 15 compounds with $AC_{50} \leq 10$ μ*M* were identified and 14 are annotated as βAR antagonists and one annotated as an α-adrenergic receptor antagonist. Twenty antagonists were not identified at the 10 μ*M* AC_{50} threshold, and 19 are annotated as specific for the α-adrenergic subtypes. Taken together, these results show that the pharmacology for a large number of known adrenergic ligands was defined accurately in these assays.

Theoretically, the antagonist assay can be used to identify both agonists and antagonists. However, we found that the antagonist screen did not identify βAR agonists as efficiently as the agonist screen. For example, the potent βAR agonist isoproterenol had a 16 n*M* AC_{50} in the agonist format but showed only a shallow increase in activation over the stimulated signal in the antagonist format (data not shown). Therefore, to ensure accurate identification of both agonists and antagonists, both formats of the assay should be performed.

FIG. 9. Validation screens of the LOPAC library against the βARR:β2AR assay. Heat maps (left) and three-dimensional scatter plots (right) of the screens against the agonist (A) and antagonist (B) formats of the βARR:β2AR assay. The LOPAC collection was screened at 15 concentrations, and five DMSO plates were included for background correction. Heat maps show carryover of some potent library compounds into the DMSO plates. Three-dimensional scatter plots indicate inactive samples (black) and active (agonist, red; antagonist, blue) samples that showed a concentration–response relationship.

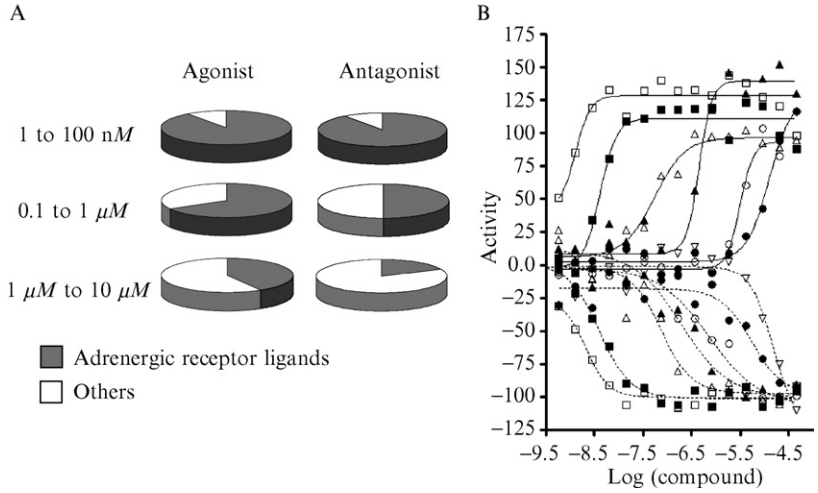

FIG. 10. Results of the LOPAC screen against the βARR:β2AR assay. (A) LOPAC annotation of compounds binned by the AC_{50} identified in the agonist format, 1 to 100 nM ($n = 10$), 0.1 to 1 μM ($n = 9$), and 1 to 10 μM ($n = 12$), and the antagonist format, 1 to 100 nM ($n = 10$), 0.1 to 1 μM ($n = 25$), and 1 to 10 μM ($n = 44$). (B) Example concentration–response curves of agonists (solid lines), LOPAC-F-9552 (formoterol, □), LOPAC-I-6504(isoproterenol, ■), LOPAC-S-8260 (albuterol, △), LOPAC-E-4642 [(±)-epinephrine, ▲], LOPAC-A-0966 (4-amino-1,8-naphthalimide, ○), and LOPAC-S-8442 (1,3-dihydro-3-[3,5-dimethyl-1*H*-pyrrol-2-yl], ●), and antagonists (dotted lines), LOPAC-P-152 [*S*(−)-pindolol, □], LOPAC-P-0884 [(±)-propranolol, ■], LOPAC-L-1011 (labetalol, △), LOPAC-B-5683 (betaxolol, ▲), LOPAC-P-4670 (propafenone, ○), LOPAC-C-106 (7-trifluoromethyl-4 (4-methyl-1-piperazinyl)-pyrrolo[1,2-a]quinoxaline, ●), and LOPAC-T-1132 (tetraethylthiuram disulfide, □), are shown.

Summary

Optimal assay performance with the Acumen Explorer requires reducing background fluorescence, maximizing signal, and choosing the proper cell density and object characteristics. We found that the greatest improvement in assay quality was achieved by lowering background fluorescence. This was accomplished by washing adherent cells in the case of the GR-GFP and LDR assays. For weakly adherent cells, as in the βARR:β2AR assay, the fluorescence-absorbing dye naphthol blue black was added to the wells.

Microtiter plate laser-scanning cytometry is a powerful technology enabling cellular analysis similar to that of conventional flow cytometry. While the plate-based method described here has fewer excitation and emission channels compared to flow cytometry [up to 17 colors can be

detected (Perfetto *et al*., 2004)], the system has important advantages for compound screening. This technique can detect fluorescent signals from adherent cells, which are the basis of numerous assays used in screening. In addition, microtiter plate cytometers can be integrated easily with standard robotic screening systems, enabling the screening of large compound libraries at greater than 200,000 samples per day.

The application of microplate cytometers can be enhanced if used in conjunction with CCD-based microscope systems by integrating both components into a screening process. In this scenario, a microplate cytometer identifies active wells in high-throughput mode; these wells are subsequently imaged at high resolution using a CCD-based microscope. In the case of GR-GFP, a microplate cytometer would identify actives based on cytosol-to-nuclear translocation, whereas a microscope-based imager would classify actives by more subtle patterns of nuclear sublocalization. It is known that different ligands cause distinct distributions of GR into nuclear subdomains (Htun *et al*., 1996). Development of such integrated detection systems should increase the variety of phenotypic assays applied to HTS systems.

Acknowledgments

We gratefully acknowledge Dr. Pagliaro of BioImage for providing the GR-GFP cell line for this study and Eric Sprigg of TTP Labtech for technical assistance with the Acumen Explorer. This research was supported by the NIH Roadmap for Medical Research and the Intramural Research Program of the National Human Genome Research Institute, National Institutes of Health.

References

Bai, C., Schmidt, A., and Freedman, L. P. (2003). Steroid hormone receptors and drug discovery: Therapeutic opportunities and assay designs. *Assay Drug Dev. Technol.* **1,** 843–852.

Ben-Kasus, T., Ben-Zvi, Z., Marquez, V. E., Kelley, J. A., and Agbaria, R. (2005). Metabolic activation of zebularine, a novel DNA methylation inhibitor, in human bladder carcinoma cells. *Biochem. Pharmacol.* **70,** 121–133.

Bowen, W. P., and Wylie, P. G. (2006). Application of laser-scanning fluorescence microplate cytometry in high content screening. *Assay Drug Dev. Technol.* **4,** 209–221.

Carroll, S. S., Inglese, J., Mao, S.-S., and Olsen, D. B. (2004). Drug screening: Assay development issues. *In* ''Molecular Cancer Therapeutics: Strategies for Drug Discovery and Development'' (D. B. Prendergast, ed.), pp. 119–140. Wiley, Hoboken, NJ.

Cleveland, P. H., and Koutz, P. J. (2005). Nanoliter dispensing for uHTS using pin tools. *Assay Drug Dev. Technol.* **3,** 213–225.

Ferguson, S. S. G., Zhang, J., Barak, L. S., and Caron, M. G. (1998). Molecular mechanisms of G protein-coupled receptor desensitization and resensitization. *Life Sci.* **62,** 1561–1565.

Garippa, R. J., Hoffman, A. F., Gradl, G., and Kirsch, A. (2006). High-throughput confocal microscopy for β-arrestin–green fluorescent protein translocation G protein-coupled receptor assays using the Evotec Opera. *Methods Enzymol.* **414** (this volume).

Ghoshal, K., Datta, J., Majumder, S., Bai, S., Dong, X., Parthun, M., and Jacob, S. T. (2002). Inhibitors of histone deacetylase and DNA methyltransferase synergistically activate the methylated metallothionein I promoter by activating the transcription factor MTF-1 and forming an open chromatin structure. *Mol. Cell. Biol.* **22,** 8302–8319.

Haasen, D., Schnapp, A., Valler, M. J., and Heilker, R. (2006). G protein-coupled receptor internalization assays in the high-content screening format. *Methods Enzymol.* **414** (this volume).

Htun, H., Barsony, J., Renyi, I., Gould, D. L., and Hager, G. L. (1996). Visualization of glucocorticoid receptor translocation and intranuclear organization in living cells with a green fluorescent protein chimera. *Proc. Natl. Acad. Sci. USA* **93,** 4845–4850.

Inglese, J., Auld, D. S., Jadhav, A., Johnson, R. L., Simeonov, A., Yasgar, A., Zheng, W., and Austin, C. P. (2006). Quantitative high-throughput screening (qHTS): A titration-based approach that efficiently identifies biological activities in large chemical libraries. *Proc. Natl. Acad. Sci. USA* **103,** 11473–11478 .

Inglese, J., Freedman, N. J., Koch, W. J., and Lefkowitz, R. J. (1993). Structure and mechanism of the G protein-coupled receptor kinases. *J. Biol. Chem.* **268,** 23735–23738.

Jung-Testas, I., and Baulieu, E. E. (1983). Inhibition of glucocorticosteroid action in cultured L-929 mouse fibroblasts by RU 486, a new anti-glucocorticosteroid of high affinity for the glucocorticosteroid receptor. *Exp. Cell Res.* **147,** 177–182.

Levinson, B. B., Baxter, J. D., Rousseau, G. G., and Tomkins, G. M. (1972). Cellular site of glucocorticoid-receptor complex formation. *Science* **175,** 189–190.

MacDonald, M. L., Lamerdin, J. L., Owens, S., Keon, B. H., Bilter, G. K., Shang, Z., Huang, Z., Yu, H., Dias, J., Minami, T., Michnick, S. W., and Westwick, J. K. (2006). Identifying off-target effects and hidden phenotypes of drugs in human cells. *Nature Chem. Biol*.

Mainquist, J. K. D., Robert, C., Weselak, M. R., Meyer, A. J., Burow, K. M., Sipes, D. G., and Caldwell, J. (2003). Specimen plate lid and method of using. U.S. Patent #6534014.

Martinez, E. D., Rayasam, G. V., Dull, A. B., Walker, D. A., and Hager, G. L. (2005). An estrogen receptor chimera senses ligands by nuclear translocation. *J. Steroid Biochem. Mol. Biol.* **97,** 307–321.

Martinez, E. D., Dull, A. B., Beutter, J. A., and Hager, G. L., (2006). High content fluorescene-based screening for epigenetic modulators. *Methods Enzymol.* **414,** 21–36.

Niles, W. D., and Coassin, P. J. (2005). Piezo- and solenoid valve-based liquid dispensing for miniaturized assays. *Assay Drug. Dev. Technol.* **3,** 189–202.

Perfetto, S. P., Chattopadhyay, P. K., and Roederer, M. (2004). Seventeen-colour flow cytometry: Unravelling the immune system. *Nature Rev. Immunol.* **4,** 648–655.

Remy, I., and Michnick, S. W. (2003). Dynamic visualization of expressed gene networks. *J. Cell Physiol.* **196,** 419–429.

Richards, G. R., Jack, A. D., Platts, A., and Simpson, P. B. (2006). Measurement and analysis of calcium signaling in heterogeneous cell cultures. *Methods Enzymol.* **414,** 335–347.

Shaner, N. C., Steinbach, P. A., and Tsien, R. Y. (2005). A guide to choosing fluorescent proteins. *Nature Methods* **2,** 905–909.

Thiagalingam, S., Cheng, K. H., Lee, H. J., Mineva, N., Thiagalingam, A., and Ponte, J. F. (2003). Histone deacetylases: Unique players in shaping the epigenetic histone code. *Ann. N.Y. Acad. Sci.* **983,** 84–100.

van Roessel, P., and Brand, A. H. (2002). Imaging into the future: Visualizing gene expression and protein interactions with fluorescent proteins. *Nature Cell Biol.* **4,** E15–E20.

Williams, R. G., Kandasamy, R., Nickischer, D., Trask, O. J., Laethem, C., Johnston, P. A., and Johnston, P. A. (2006). Generation and characterization of a stable MK2-EGFP cell line and subsequent development of a high-content imaging assay on the Cellomics ArrayScan platform to screen for p38 mitogen-activated protein kinase inhibitors. *Methods Enzymol.* **414** (this volume).

Yu, H., West, M., Keon, B. H., Bilter, G. K., Owens, S., Lamerdin, J., and Westwick, J. K. (2003). Measuring drug action in the cellular context using protein-fragment complementation assays. *Assay Drug Dev. Technol.* **1,** 811–822.

Zhou, J., and Cidlowski, J. A. (2005). The human glucocorticoid receptor: One gene, multiple proteins and diverse responses. *Steroids* **70,** 407–417.

[30] High-Throughput Measurements of Biochemical Responses Using the Plate::Vision Multimode 96 Minilens Array Reader

By KUO-SEN HUANG, DAVID MARK, and FRANK ULRICH GANDENBERGER

Abstract

The plate::vision is a high-throughput multimode reader capable of reading absorbance, fluorescence, fluorescence polarization, time-resolved fluorescence, and luminescence. Its performance has been shown to be quite comparable with other readers. When the reader is integrated into the plate::explorer, an ultrahigh-throughput screening system with event-driven software and parallel plate-handling devices, it becomes possible to run complicated assays with kinetic readouts in high-density microtiter plate formats for high-throughput screening. For the past 5 years, we have used the plate::vision and the plate::explorer to run screens and have generated more than 30 million data points. Their throughput, performance, and robustness have speeded up our drug discovery process greatly.

Introduction

In the mid- to late 1990s pharmaceutical companies began to invest heavily in high-throughput screening (HTS) technologies to speed up their drug discovery processes. Early HTS platforms, typically built around track-mounted articulate robots, could handle just one task at a time and achieve throughputs of only 20,000 compounds per day. They were not fast enough to keep pace with the increasing size of compound libraries and number of screening targets. Furthermore, because many of them could

METHODS IN ENZYMOLOGY, VOL. 414 0076-6879/06 $35.00

DOI: 10.1016/S0076-6879(06)14030-6